HHS Public Access

Author manuscript

Nat Biotechnol. Author manuscript; available in PMC 2016 June 14.

Published in final edited form as:

Nat Biotechnol. 2016 February ; 34(2): 164–166. doi:10.1038/nbt.3427.

Antisense-oligonucleotide-directed inhibition of nonsense-mediated mRNA decay

Tomoki T. Nomakuchi[1,2], **Frank Rigo**[3], **Isabel Aznarez**[1], and **Adrian R. Krainer**[1]

[1]Cold Spring Harbor Laboratory, Cold Spring Harbor, New York, USA

[2]Stony Brook University School of Medicine, Stony Brook, New York, USA

[3]Isis Pharmaceuticals, Carslbad, California, USA

Abstract

Nonsense-mediated mRNA decay (NMD) is a cellular quality-control mechanism that is thought to exacerbate the phenotype of certain pathogenic nonsense mutations by preventing the expression of semi-functional proteins. NMD also limits the efficacy of read-through compound (RTC)-based therapies. Here, we report a gene-specific method of NMD inhibition using antisense oligonucleotides (ASOs), and combine this approach with an RTC to effectively restore the expression of full-length protein from a nonsense-mutant allele.

RNA-based therapeutic approaches have become increasingly promising, as exemplified by the recent progress in the development of ASOs and stop-codon RTCs as therapeutics for various genetic diseases[1,2]. NMD is a quality-control process that degrades mRNAs with premature termination codons (PTCs) during translation[3]. mRNAs targeted by small molecules that allow the ribosome to read-through stop codons are often subject to NMD, reducing the therapeutic potential of such RTCs[4]. NMD suppression has thus gained attention as a potential RNA-based therapy, but the proposed approaches so far have relied on general inhibition of the NMD machinery[5–7]. Transcript-specific, as opposed to global, inhibition of NMD is desirable, because in addition to its protective role from the potential toxicity of certain truncated proteins, NMD plays an important role in global post-transcriptional gene regulation, for example, by alternative splicing coupled with NMD[8,9]. Indeed, NMD plays essential roles in development, such as in myogenesis, neurogenesis and lymphocyte maturation[1]. For example, UPF3B, a key regulator of NMD, is necessary for neural-progenitor cell differentiation and is mutated in various cognitive disorders[10].

Correspondence should be addressed to A.R.K. (; Email: krainer@cshl.edu) or I.A. (; Email: aznarez@cshl.edu)

Author contributions

T.T.N., I.A. and A.R.K. designed the experiments. I.A. and F.R. provided critical reagents. T.T.N. performed the research. T.T.N. and A.R.K. wrote the manuscript. All authors approved the manuscript.

Competing Financial Interests

F.R. is an employee of, and A.R.K. is a consultant for, Isis Pharmaceuticals. A.R.K., I.A., and T.T.N. are inventors in a related patent application, PCT/US2014/054151.

NMD relies on the presence of at least one exon-junction complex (EJC) bound to the mRNA downstream of a PTC. During translation, when a ribosome reaches a PTC, it associates with the release factors eRF1 and eRF3, and interacts with the downstream EJC through UPF1, UPF2, and UPF3A/3B proteins[1]. This physical interaction provides a platform to recruit additional NMD factors, targeting the mRNA for destruction. Given that most EJCs are assembled 20–24 nucleotides upstream of each exon-exon junction during splicing, and that the EJC is not required for splicing of most exons, we have developed an antisense approach that takes advantage of the predictable nature of EJC deposition[11].

ASOs can be designed to block the binding sites of RNA-binding proteins, resulting in effects such as splicing modulation and inhibition of translation initiation, among others[12]. We tested whether ASOs can be used for targeted NMD inhibition by blocking EJC deposition on mRNA, downstream of a PTC. Although EJCs appear to be dispensable for most splicing events, they have roles in mRNP export from the nucleus and in translation[13]. Our approach is not expected to affect such processes, because we only target EJCs downstream of a PTC on a given mRNA, leaving the remaining upstream EJCs unaffected.

We first tested a well-characterized NMD substrate, the full-length three-exon *HBB* (β-globin) gene with the Q39X nonsense mutation (CAG→TAG) in exon 2 (*HBB*-T39)[14]. We stably expressed a single copy of this gene, following Flp-recombinase-mediated integration at a defined site in U2OS T-REx cells. In this context, *HBB*-T39 mRNA expression was reduced to about 5% compared to wild type *HBB* (Supplementary Fig. 1). We designed a set of 2′-*O*-(2-methoxyethyl) ribose (MOE) and phosphorothioate modified 15mer ASOs that together span the region of the *HBB*-T39 mRNA predicted to harbor an EJC, and screened them individually for NMD-inhibiting activity (Fig. 1a, b). After transfection, many of the ASOs caused skipping of *HBB* exon 2; however, several ASOs resulted in minimal exon skipping, and markedly increased the level of full-length spliced mRNA (Fig. 1c and Supplementary Fig. 2). We chose H-24 as the lead ASO, and confirmed its dose-dependent activity, which resulted in a 3-fold increase in *HBB*-T39 mRNA at the highest dose tested (Fig. 1d). Consistent with NMD inhibition, H-24 did not affect the levels of wild-type *HBB* mRNA (Supplementary Fig. 3). To verify the transcript-specific effect of NMD-inhibiting ASOs, we confirmed that the expression of several NMD-targeted endogenous mRNAs remained unchanged following ASO treatment (Supplementary Fig. 4)[15].

To test the generality of our approach, we constructed a three-exon NMD minigene reporter based on the *MECP2* gene with the S65X nonsense mutation (TCA→TGA) in the middle exon (exon 3 in the natural gene), similarly integrated at a defined location in U2OS T-REx cells. *MECP2*-S65X mRNA was efficiently degraded by NMD (Supplementary Fig. 5). We screened a corresponding set of 19 ASOs spanning the presumptive EJC binding site near the 3′ end of this exon and identified multiple ASOs that increased the amount of full-length spliced mRNA (Supplementary Fig. 6). One of several effective ASOs for *MECP2* (M-33) resulted in a ~3-fold increase in mRNA (Fig. 1e).

The above NMD substrates are simple three-exon genes or minigenes with a single predicted EJC downstream of a PTC. To test the broader applicability of our approach, we designed a pair of four-exon hybrid genes, consisting in one case of *HBB* exons 1 through 3, with exon

3 and portions of the flanking introns from *MECP2* inserted within *HBB* intron 2, and in the other case of *MECP2* exons 2 through 4, with *HBB* exon 2 and portions of the flanking introns inserted within *MECP2* intron 3 (Fig. 1f and Methods). Using our optimal ASOs for these two genes (H-24 for *HBB* and M-33 for *MECP2*), we compared the effects of single and combined ASOs in inhibiting NMD of these target substrates with two presumptive downstream EJCs. In both cases, the combined treatment with both ASOs was more effective than with either ASO alone (Fig. 1g, Supplementary Fig. 7).

NMD is sensitive to the cellular state and environment, and can be inhibited by stress, e.g., hypoxia and amino-acid deprivation[16]. Furthermore, ASOs can have various off-target effects, although none has been linked to NMD efficiency[17]. To test the presumptive mechanism of action, we performed *in vitro* splicing followed by GST-eIF4A3 pull-down to confirm that an effective ASO blocks the interaction between the spliced mRNA and eIF4A3, the anchor component of the EJC[18]. Consistent with its predicted activity, H-24 ASO blocked the interaction between *HBB* mRNA and eIF4A3 in a dose-dependent manner (Fig. 2a).

To further establish the mechanism of action, we modified the *HBB*-T39 construct by adding 24 nucleotides at the 3′ end of exon 2. Due to the position-specific nature of EJC binding, this modification shifts the predicted EJC-deposition site downstream of the sequence targeted by H-24 ASO (Fig. 2b)[1, 18]. The mRNA expressed from this construct (*HBB*-T39+24) was not affected by H-24, indicating that the ASO target sequence has to overlap with the predicted EJC-assembly site to inhibit NMD (Fig. 2c).

Additionally, to rule out the possibility that the increase in steady-state mRNA level reflects an increased rate of transcription, we performed an actinomycin D chase assay to measure the mRNA decay rate. As expected, cells treated with H-24 ASO expressed *HBB*-T39 mRNA with greater stability (Supplementary Fig. 8). *HBB*-T39 mRNA was reported to undergo biphasic decay, likely due to rapid decay of the NMD-sensitive mRNA molecules, occurring alongside slower decay of a subset of mRNA molecules that evade NMD[19]. Analysis of the half-lives in two phases revealed that the stability of *HBB-T39* mRNA in ASO-treated cells was higher during the rapid-decay phase (estimated $t_{1/2}$ = 6.8 min untreated vs. 16.5 min ASO-treated), whereas the decay rate during the slow phase remained unchanged (estimated $t_{1/2}$ > 12 hr for both treatment groups).

To determine if the target-mRNA increase results in an increase in the encoded protein after ASO treatment, we monitored the effect of ASO on protein synthesis, via a GFP tag placed at the N-terminus of *HBB*-T39. We observed a robust increase in the amount of truncated protein in response to ASO treatment (Supplementary Fig. 9). Notably, ASO treatment did not reduce the amount of full-length protein expressed from the wild-type GFP fusion construct (Supplementary Fig. 10). We conclude that protein synthesis is not inhibited by an exon-targeting MOE phosphorothioate ASO, presumably because it is displaced from the mRNA upon passage of a translating ribosome.

RTCs are diverse classes of molecules that cause the ribosome to misrecognize a PTC and incorporate an amino acid, terminating at the natural stop codon downstream, and thereby

restoring synthesis of full-length protein from mRNA with a nonsense mutation[20]. Although this is a promising strategy currently being tested in clinical trials, NMD diminishes the efficacy of read-through therapy by degrading the mRNAs targeted by such compounds[4,5].

To test the utility of our approach in improving the efficacy of RTCs, we designed a read-through reporter, *HBB*-T39(UGAC), based on the above GFP-tagged *HBB*-T39 construct, by replacing the TAG PTC and the following four nucleotides with TGACTAG. This stop codon and the downstream sequence weaken translation termination, allowing some spontaneous read-through, and thereby increasing the sensitivity of detection of full-length protein[21]. Translational read-through suppresses NMD to some extent, as is evident by the 2–3 fold increase in *HBB*-T39(UGAC) mRNA, relative to *HBB*-T39 (Supplementary Fig. 1). Nevertheless, we observed strong increases in both the truncated protein and the read-through product upon further NMD suppression by H-24 ASO treatment (Fig. 2d and Supplementary Fig. 11).

G418 is an aminoglycoside with read-through activity[4]. Co-treatment of U2OS cells expressing *HBB*-T39(UGAC) with H-24 ASO and G418 increased the full-length protein level by 6-fold, compared to a 2-fold increase with G418 alone, and a 2.5-fold increase with H-24 ASO alone. Thus, antisense inhibition of NMD can augment the efficacy of a read-through compound. The ASO-induced increase in expression of truncated protein could be deleterious in some cases, but this would depend on the properties of the particular mutant protein, and on the efficacy of the RTC.

The antisense approach we present here, which we dubbed GAIN (for Gene-specific Antisense Inhibition of NMD) allows gene-specific inhibition of NMD without relying on skipping of a PTC-containing exon. This gene-specific feature, along with the clinically demonstrated efficacy and safety profiles of various ASO chemistries, such as MOE phosphorothioate, makes this a promising approach to inhibit NMD[2].

Methods

ASOs

All ASOs used were uniformly modified with 2′O-MOE sugars, phosphorothioate backbone, and 5′-methyl cytosine. Synthesis, purification, and quantitation were done as described[22]. All ASOs were dissolved in water and stored at −20°C. The sequences of all ASOs used in this study are provided in Supplementary Table 1. ASOs were named by taking the first letter of their target gene, followed by a number representing the distance of the ASO 5′ end from the exon-exon junction.

Preparation of NMD reporter cells

All the cell lines used in this study tested negative for mycoplasma contamination. The full *HBB* gene and *MECP2* exons 2 to 4 were cloned into the pcDNA FRT/TO plasmid (Life Technologies), with GFP sequence at the 5′ end of the first exon for monitoring protein expression. Only 200 bases at each end of *MECP2* intron 3 (59,626 nt) were included in the construct. Chimeric constructs were made as follows: for Construct 1, *MECP2* exon 3, along with the last 173 nt of intron 2 and the first 145 nt of intron 3, was inserted into *HBB* intron

2 at position IVS2+473. Likewise, for Construct 2, *HBB* exon 2, along with the last 60 nt of intron 1 and the first 79 nt of intron 2, was inserted into *MECP2* intron 3 at position IVS3+335. Cloning was carried out by the sequence- and ligation-independent cloning strategy (SLIC)[23], and PTCs were introduced by site-directed mutagenesis. *HBB*-T39+24 was made from *HBB*-T39 by replacing 6 nt at the 3′ end of *HBB* exon 2 with 30 nt from the 3′ end of *HBB* exon 1. The pcDNA FRT/TO constructs were co-transfected along with pOG44 helper vector into FRT-U2OS-TRex cells with a single integration site (Life Technologies). Cells with successful FRT-mediated integration were obtained by hygromycin selection. The expression and correct splicing of the transgenes were confirmed by radioactive RT-PCR, following induction with 1 μg/ml tetracycline.

Tissue culture and ASO transfection

U2OS cells were cultured in DMEM with 10% FBS. ASO transfections were carried out using Lipofectamine 2000 (Life Technologies) according to the manufacturer's protocol for transfecting short oligonucleotides. Transgenes were induced with 1 μg/ml tetracycline, 6 hr after transfection. For the G418-treatment group, G418 (Sigma) was added at a final concentration of 1 mg/ml at the time of transgene induction, and again during a change of medium 24 hr after transfection.

RNA extraction and RT-PCR

Total RNA was extracted with TRIzol (Life Technologies) 48 hr post-transfection, according to the manufacturer's protocol. Oligo dT(18)-primed reverse transcription was carried out with ImpromII Reverse Transcriptase (Roche). Semi-quantitative RT-PCR was carried out in the presence of ^{32}P-dCTP and primer pairs corresponding to the first and last exons of each construct. *MECP2* cDNA was amplified using a forward primer specific to GFP sequence, to avoid detecting the endogenous wild-type *MECP2* mRNA. Primer sequences are provided in Supplementary Table 2. PCR products were detected with a Typhoon FLA7000 phosphorimager, and quantitated using MultiGauge v2.3 software (Fujifilm). Statistical significance was calculated using Student's *t*-test.

Protein extraction and Western blotting

Cells were harvested 48 hr after transfection and lysed in STEN lysis buffer (50 mM Tris, pH 7.6, 150 mM NaCl, 0.1% SDS, 1% NP-40, and 2 mM EDTA + protease inhibitor cocktail (Roche)) by sonicating for 5 min at medium power using a Bioruptor (Diagenode), followed by 15-min incubation on ice. Protein concentration was measured using the Bradford assay (Bio-Rad) with BSA as a standard. Rabbit anti-GFP (Sigma G1544) and mouse anti-α-tubulin (Sigma T9026) antibodies were used with IRDye 800CW secondary antibodies (LI-COR) for Western blotting, and the blots were imaged and quantified using the Odyssey Infrared Imaging System (LI-COR).

In vitro transcription of *HBB* minigene

Pre-mRNA for *in vitro* splicing was transcribed using T7 RNA polymerase (Roche) in the presence of α-^{32}P-UTP, using a PCR product as the template. The template contains portions of exons 2 and 3 and the intact intron 2 of *HBB*, and was amplified from human genomic

DNA using the primer pair T7HBB-Ex2-F and HBB-Ex3-R (Supplementary Table 2). The radiolabeled transcript was purified by denaturing PAGE, and its concentration measured by liquid scintillation counting.

In vitro splicing and GST pull-down

Expression and purification of GST-eIF4A3, HeLa nuclear extract preparation, and *in vitro* splicing were carried out essentially as described[18, 24, 25]. 50-μl splicing reactions were carried out for 90 min at 30 °C with 4 μg of GST alone or GST-eIF4A3, in the presence of varying concentrations of ASOs. A 5-μl aliquot was kept as input, and 400 μl of wash buffer (20 mM Hepes, pH 8.0, 150 mM KCl, 0.05 % NP-40) was added to the remainder. mRNP was bound to 10 μl of glutathione-Sepharose beads (GE Healthcare) by nutating at 4 °C for 2 hr. The beads were washed three times with wash buffer, and resuspended in 300 μl of splice-stop solution (0.3 mM NaOAc and 0.1% SDS). RNA was then recovered by phenol extraction and ethanol precipitation, and analyzed by denaturing PAGE, followed by detection and quantitation on a Typhoon phosphorimager.

mRNA decay rate assay

U2OS cells with stably integrated *HBB*-T39 constructs were pre-treated with transfection reagent (control) or 50 nM H-24 ASO. Expression of the transgene was induced 24 hr post-transfection by addition of 1 μg/ml tetracycline. Two hours post-induction, transcription was halted by washing the cells once with PBS and replacing the medium with medium containing 5 μg/ml actinomycin D and no tetracycline. Starting 30 min after actinomycin D addition (defined as 0 hr), cells were harvested in TRIzol at the indicated time points to assess the decay rate of *HBB*-T39 mRNA. The amount of *HBB* mRNA was normalized to *ACTB* mRNA. Half-lives were calculated using the two-component mixed exponential decay model $y = a \times \exp(b \times t) + c \times \exp(d \times t)$; data from our experiment were fitted to this model using the Solver function of Microsoft Excel to solve for the decay constants b and d[19, 26].

Supplementary Material

Refer to Web version on PubMed Central for supplementary material.

Acknowledgments

We thank Frank Bennett for helpful discussions. This work was supported by NIH grants R21-NS081448 and R37-GM042699, and by a research grant from the University of Pennsylvania's Center for Orphan Disease Research and Therapy to A.R.K. We acknowledge assistance from CSHL Shared Resources, which are funded in part by Cancer Center Support Grant 5P30CA045508.

References

1. Goldmann T, et al. EMBO Mol Med. 2012; 4:1186–1199. [PubMed: 23027640]
2. Rigo F, Hua Y, Krainer AR, Bennett CF. J Cell Biol. 2012; 199:21–25. [PubMed: 23027901]
3. Popp MWL, Maquat LE. Annu Rev Genet. 2013; 47:139–165. [PubMed: 24274751]
4. Keeling KM, et al. PLoS ONE. 2013; 8:e60478. [PubMed: 23593225]
5. Keeling KM, Bedwell DM. Wiley Interdiscip Rev RNA. 2011; 2:837–852. [PubMed: 21976286]
6. Bhuvanagiri M, et al. EMBO Mol Med. 2014; 6:1593–1609. [PubMed: 25319547]

7. Martin L, et al. Cancer Res. 2014; 74:3104–3113. [PubMed: 24662918]
8. Ni JZ, et al. Genes Dev. 2007; 21:708–718. [PubMed: 17369403]
9. Karam R, Wilkinson M. RNA Biol. 2012; 9:22–26. [PubMed: 22258150]
10. Jolly LA, Homan CC, Jacob R, Barry S, Gecz J. Hum Mol Genet. 2013
11. Shibuya T, Tange TO, Sonenberg N, Moore MJ. Nat Struct Mol Biol. 2004; 11:346–351. [PubMed: 15034551]
12. Kole R, Krainer AR, Altman S. Nat Rev Drug Discov. 2012; 11:125–140. [PubMed: 22262036]
13. Giorgi C, Moore MJ. Semin Cell Dev Biol. 2007; 18:186–193. [PubMed: 17459736]
14. Trecartin RF, et al. J Clin Investig. 1981; 68:1012–1017. [PubMed: 6457059]
15. Pan Q, et al. Genes Dev. 2006; 20:153–158. [PubMed: 16418482]
16. Gardner LB. Mol Cancer Res. 2010; 8:295–308. [PubMed: 20179151]
17. Winkler J, Stessl M, Amartey J, Noe CR. ChemMedChem. 2010; 5:1344–1352. [PubMed: 20544786]
18. Zhang Z, Krainer AR. Proc Natl Acad Sci USA. 2007; 104:11574–11579. [PubMed: 17606899]
19. Trcek T, Sato H, Singer RH, Maquat LE. Genes & Development. 2013; 27:541–551. [PubMed: 23431032]
20. Keeling KM, Xue X, Gunn G, Bedwell DM. Annu Rev Genomics Hum Genet. 2014; 15:371–394. [PubMed: 24773318]
21. Loughran G, et al. Nucleic Acids Res. 2014; 42:8928–8938. [PubMed: 25013167]
22. Baker BF, et al. J Biol Chem. 1997; 272:11994–12000. [PubMed: 9115264]
23. Jeong JY, et al. Appl Environ Microbiol. 2012; 78:5440–5443. [PubMed: 22610439]
24. Mayeda A, Krainer AR. Methods Mol Biol. 1999; 118:315–321. [PubMed: 10549534]
25. Mayeda A, Krainer AR. Methods Mol Biol. 1999; 118:309–314. [PubMed: 10549533]
26. Zheng W, Finkel JS, Landers SM, Long RM, Culbertson MR. Genetics. 2008; 180:1391–1405. [PubMed: 18791219]

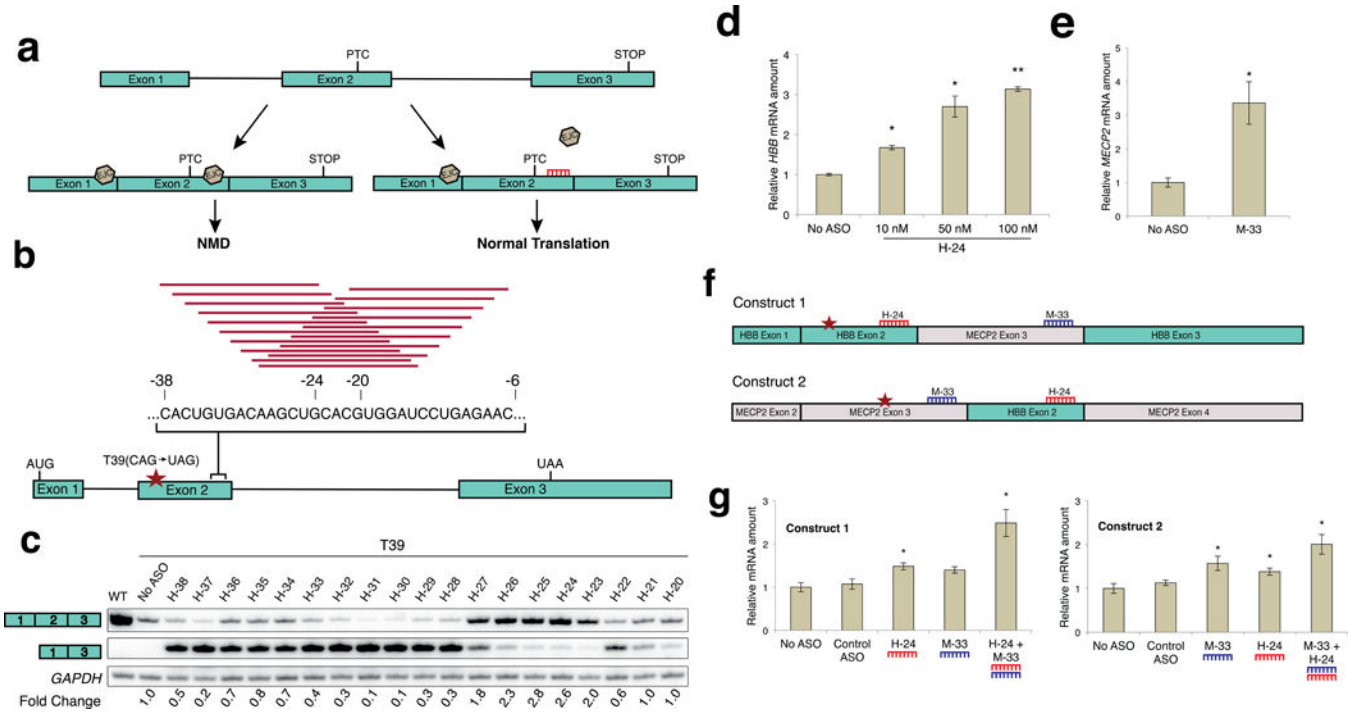

Figure 1.

Design and testing of EJC-targeting ASOs. (**a**) Schematic of the antisense approach to inhibit NMD of a target mRNA. An ASO (red) complementary to the predicted EJC-deposition site downstream of the PTC interferes with EJC assembly, inhibiting NMD. (**b**) An example of the ASO screening strategy, using *HBB* with a PTC in codon 39, stably expressed in U2OS cells. A set of 19 uniformly modified MOE phosphorothioate 15-mer ASOs was designed to cover the presumptive EJC-deposition site at 1-nt resolution. (**c**) ASOs targeting the *HBB* exon 2 EJC region were individually transfected at a nominal concentration of 100 nM. *HBB* mRNA was measured by radioactive RT-PCR using primers in exons 1 and 3. Some of the ASOs caused skipping of exon 2. The fold change in full-length mRNA with the T39 mutation, relative to the no-ASO control in lane 2, is indicated below each lane. The uncropped autoradiograph is shown in Supplementary Figure 2. (**d**) The optimal ASO for *HBB* (H-24, based on three experiments as in (c)) was tested at the indicated nominal concentrations ($n = 3$, $^{*}P < 0.05$, $^{**}P < 0.001$ versus no-ASO control). (**e**) The same screening approach was used to identify an ASO (M-33) that effectively inhibits NMD of *MECP2* mRNA with a PTC in its penultimate exon ($n = 3$). See also Supplementary Figure 3. (**f**) Constructs to test the feasibility of targeted antisense inhibition of NMD in the case of targets with more than one downstream EJC. (**g**) 50 nM of individual ASOs and 25 nM each of the combined ASOs were tested with each chimeric construct ($n = 4$). Error bars represent standard deviation (s.d.). The corresponding autoradiographs are shown in Supplementary Figure 7.

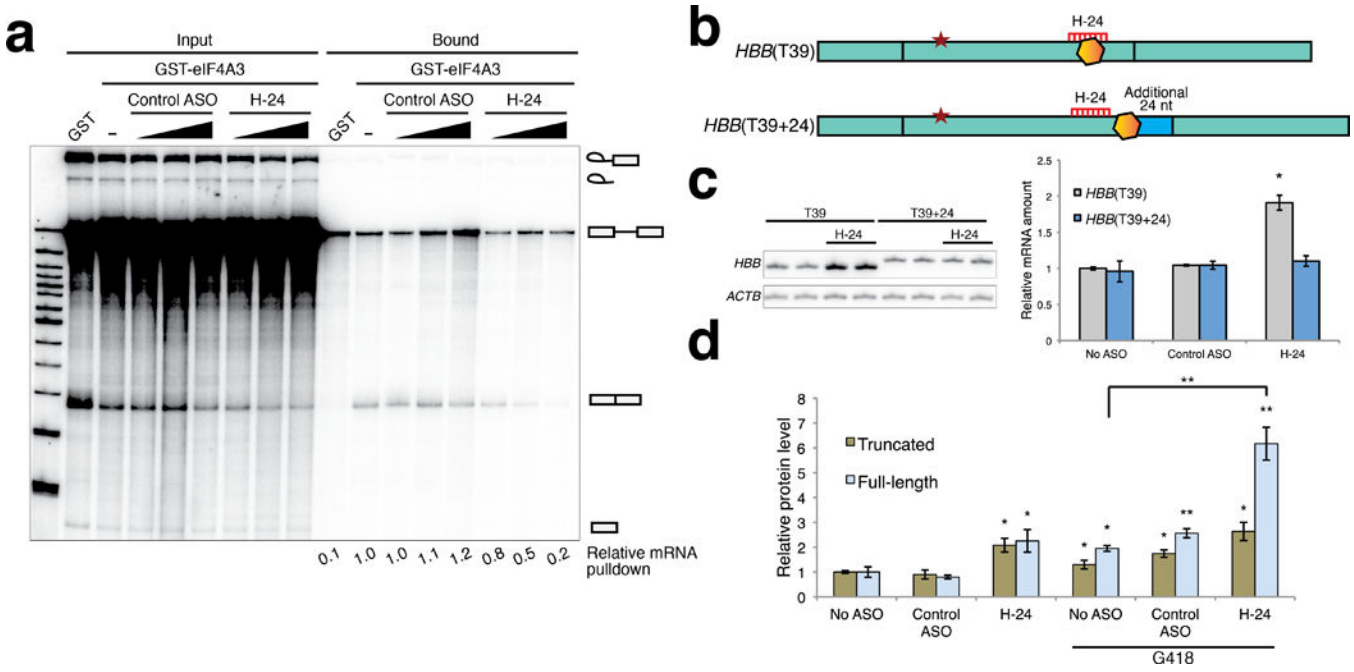

Figure 2.

Validation of the mechanism of action of NMD inhibition. (**a**) In vitro splicing of a radiolabeled pre-mRNA comprising exon 2, intron 2, and exon 3 of *HBB* was carried out in HeLa nuclear extract in the presence of GST-eIF4A3 (or GST) and varying concentrations of control or targeting ASOs. Spliced mRNA was specifically pulled down by GST-eIF4A3 in the absence of ASO or in the presence of control ASO in the splicing reaction. H-24 ASO prevented the association of eIF4A3 with the spliced mRNA in a dose-dependent manner. The relative changes in mRNA pull-down efficiency, normalized to the spliced mRNA level of the corresponding input, are indicated below each lane. 5% of the input RNA is shown on the left lanes. [ASO] = 100 nM, 200 nM, or 500 nM. (**b**) Diagram of constructs to test the dependence of the ASO effect on the position of the EJC. Addition of extra sequence (24 nt) at the end of exon 2 shifts the ASO hybridization site farther upstream from the exon-exon junction and from the site of EJC deposition. (**c**) H-24 ASO at 50 nM did not affect the NMD efficiency of the modified construct. $n = 3$, $^{*}P < 0.01$. (**d**) Antisense-inhibition of NMD increased expression of both the truncated protein and the full-length read-through product translated from a modified *HBB*-T39 mRNA that allows more efficient read-through. Expression of the full-length protein was highest when ASO (50 nM) and G-418 (1 mg/ml) were combined. The expression levels of truncated and full-length proteins are normalized to their levels in the ‘no ASO’ samples. See also Supplementary Figure 11 for a representative blot. Student’s *t*-test, * $P < 0.05$, ** $P < 0.001$; $n = 3$. Error bars represent ± s.d.